# Quartz Dissolution Kinetics from 100–200°C as a Function of pH and Ionic Strength

**W. G. Worley, J. W. Tester, and C. O. Grigsby**
Chemical Engineering Dept. and Energy Lab., Massachusetts Institute of Technology, Cambridge, MA 02139

*Of importance to geothermal energy development, oil, gas and mineral recovery, and waste storage is the characterization of the dissolution rate of host reservoir rock as a function of temperature, pressure and liquid-phase composition. As a major constitutive mineral in natural geologic systems, quartz was selected for study. Dissolution experiments were carried out in a continuous-flow, titanium autoclave reactor system at 100 – 200°C in various chemical environments. Acidification to pH 1.1 using nitric acid showed very little effect on the quartz dissolution rate. The effect of hydroxide ion concentration and ionic strength were evaluated in NaOH, NaOH/NaCl and $NaOH/Na_2SO_4$ solutions. The fractional-order dependency of the quartz dissolution rate on hydroxide ion and sodium ion (or ionic strength) concentration was determined in NaOH/NaCl solutions. The results that extend the available range of kinetic data for quartz generally agree with previous work. The observed fractional-order kinetics were qualitatively described using classical adsorption isotherms. No significant variation in the apparent reaction order of the hydroxide ion with increasing temperature could be determined due to the scatter in the data. Quartz dissolution rates were slower by about 40% in $NaOH/Na_2SO_4$ solutions than in NaOH/NaCl solutions at sodium concentrations higher than 0.01 molal. The apparent activation energy from 100 to 200°C in NaOH/NaCl solutions up to 0.01 molal hydroxide ion and 0.1 molal sodium ion was estimated to be 72 ( ± 6) kJ/mol.*

## Introduction

Rock-water interactions are important in a wide variety of geologic environments. Researchers have been motivated either because of their interest in understanding important natural geologic processes or because of a need to quantify dissolution rates for chemical processes above ground or for subsurface activities including petroleum and mineral recovery, waste isolation, and geothermal energy extraction using heat mining concepts. The motivation for carrying out this particular project was driven by engineering issues related to mineral transport in circulating hot dry rock (HDR) geothermal systems (Armstead and Tester, 1987; Charles et al., 1979; Grigsby et al., 1989; Tester et al., 1977). Of critical importance to HDR is the characterization of the rate of dissolution of host reservoir rock as a function of temperature and solution composition. In general, quartz is a major, highly reactive mineral component in HDR reservoirs in low permeability crystalline rock (Charles, 1979).

Tester et al. (1994) correlated their data with the available literature data on quartz dissolution rates in pure, deionized water from 25 to 625°C. While this treatment provides a good empirical correlation of dissolution rates in pure water from twelve different investigations, natural geothermal environments consist of widely varying solution compositions.

Most of the previous studies investigating the pH effect on the dissolution rate of quartz (Kamiya et al., 1974; Wollast and Chou, 1986; Knauss and Wolery, 1988; Grigsby, 1989; Brady and Walther, 1990; House and Orr, 1992) were limited to temperatures from 25 to 90°C. These low temperature studies show a large increase in dissolution rate as the pH is raised above pH 6, while below pH 6, the dissolution rate is nearly independent of pH. Only a few experimental studies have indicated a significant increase in rate as pH is lowered below 3 (Kamiya et al., 1974; Kline and Fogler, 1981a,b;

Correspondence concerning this article should be addressed to J. W. Tester.
Current address of C. O. Grigsby: Materials Science and Technology Division, Los Alamos National Laboratory, Los Alamos, NM 87545.

Grigsby, 1989). Kline and Fogler (1981a,b) found that the presence of strong acids and salts catalyze the dissolution rate of quartz in HF solutions. Care must be taken in comparing work performed by different investigators, since some of the low temperature experiments were conducted at constant ionic strengths, some controlled pH using variable ionic strength buffers, while others simply add acids or bases to adjust pH.

More recently, high-temperature studies have been published. Dove and Crerar (1990) performed quartz dissolution experiments in 0 to 0.15 molal (mol/kg $H_2O$) solutions of NaCl, KCl, LiCl, $MgCl_2$, and found that in all cases the presence of electrolyte increased the rate above the values measured in deionized water. However, the effect of electrolytes may be different when acids or bases are added to the solution. The effect of pH and ionic strength has been studied by Gratz and coworkers (1990, 1993) using "negative crystal" etching experiments at 166°C and 211°C. This technique has the advantage of measuring rates in specific crystal planes, however, it is limited to conditions that produce well-defined etch pits and reasonable wall retreat rates. In a recent study, Dove (1994) significantly increased the understanding of high-temperature dissolution of quartz. Data were obtained from 150 to 250°C under acidic to basic conditions and over a range of ionic strengths. Dove correlated these data with previous work and presented a model fitted to 271 data points from 25 to 300°C for solution $pH_T$ ranging from 2 to 12 and from 0 to 0.3 molal in sodium ion. The rate equation is based upon a surface reaction model that correlates changes in simulated surface complexes with quartz reactivity in aqueous solutions.

The primary objective of our work was to quantify the effects of pH and ionic strength on the dissolution rate of quartz and compare these data with previous studies. Specifically, the effect of adding acids, bases, and salts on the rate of quartz dissolution was studied. Three types of experiments were carried out: (1) the effects of $HNO_3$ and NaOH at temperatures from 100 to 200°C with no salt present; (2) the effects of NaOH at 150°C with NaCl used to maintain a constant sodium concentration (constant ionic strength); and (3) the effects of added NaCl and $Na_2SO_4$ with NaOH added to maintain a constant $OH^-$ concentration (see, for example, Dove and Rimstidt (1994) for more information on this approach).

## Experimental Methods

A commercially pure titanium autoclave reactor was constructed to allow operation up to 200°C and 600 psig (4.1 MPa) using two different mixing modes. Both modes feature a basket which holds the mineral samples in the annular space between two highly perforated cylinders with 50 mesh titanium screen secured. The first (or spinning basket) mode supports the basket on a stirring shaft to achieve the desired mixing, which is identical to setup discussed in Tester et al. (1994). The stationary basket (or spinning impeller) mode shown in Figure 1 was developed to minimize the wear on the bushings in the magnetic drive unit. In this mode, an axial-flow impeller provides the mixing, forcing fluid to flow down into the basket. The bottom of the basket is sealed, so the fluid must flow out through the basket radially. Both

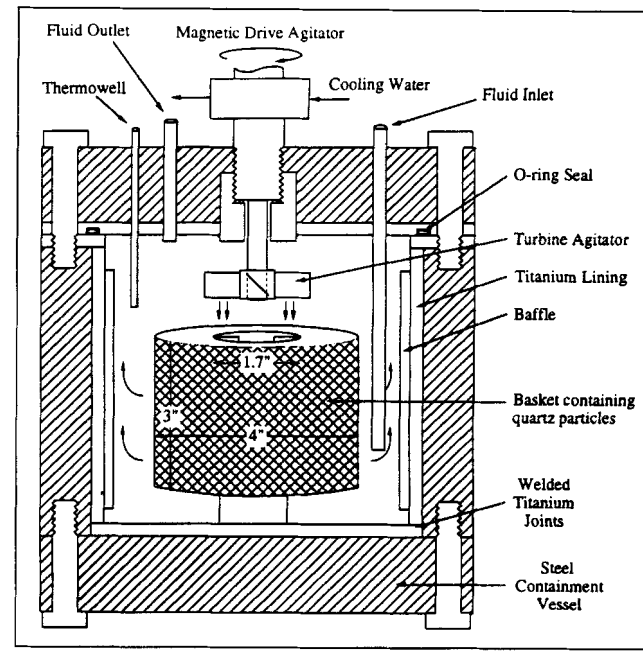


**Figure 1. Titanium stationary basket continuous-flow stirred tank reactor.**

modes approximate an ideal continuous-flow stirred tank reactor (CSTR), as verified by residence time distributions. Figure 2 shows the residence time distribution from a step change in normalized feed concentration from 0 to 1. The resulting response yields excellent agreement with the theoretical performance of a perfectly backmixed CSTR.

Quartz samples were pretreated in the reactor with deionized water at 150 to 200°C until the dissolution rate decreased to a constant value over time, thus removing all of

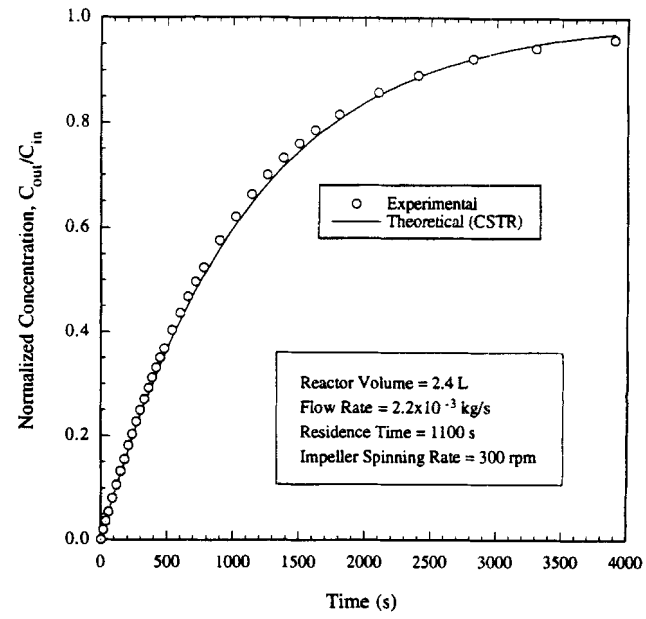


**Figure 2. Tracer-determined residence time distribution for the upgraded *Spinning Basket* reactor with rotating impeller (this study).**

**Table 1. Particle Characterization Data for Quartz Dissolution Rate Studies**

| Quartz Source | Particle Size ($\mu$m) | Specific Surface Area: Geometric ($cm^2/g$) | Specific Surface Area: BET ($cm^2/g$) |
|---|---|---|---|
| Ottawa Sand | 590–850 | 32 | 225 |
| Crushed Quartz, Hot Springs, AR | 2,380–4,000 | 7.3 | 40 |

the attached fines and "high energy" sites from the surface. All of quartz dissolution rate experiments used Ottawa sand particles except one set of experiments which used crushed quartz from Hot Springs, AR. The particle-size distributions and surface area estimates are listed in Table 1. The particle-size distributions are based on the mesh sizes of the sieves used to segregate the different size particles. The geometric surface area is calculated from the particle-size distribution assuming that the particles are smooth spheres, see Tester et al. (1994) for details. The BET values were measured by Micromeritics using krypton adsorption.

Surface preparation methods are described by Tester et al. (1994). Aqueous silica or silicic acid concentration was measured using the molybdate blue method following the ASTM standard technique #D859. Inductively coupled plasma (ICP) emission spectroscopy was used to cross-check the molybdate technique to ensure that silica polymerization was not significantly affecting the determination of dissolved $SiO_2$ (Tester et al., 1994). Dissolution rates were calculated from the measured concentrations of dissolved species in solution and the solution flow rate through the reactor, as described in the next section.

## Dissolution Rate Determination

Dissolution rate constants ($k_f$) were determined from the raw experimental data using the correlating rate Eq. 7a from Tester et al. (1994):

$$k_f = \frac{r_{\text{net}}}{\frac{A_s}{M_w}\left(1 - m_{H_4SiO_4}/m^{\text{sat}}_{H_4SiO_4}\right)} \tag{1}$$

Similar equations have been used by many previous investigators (O'Connor and Greenberg, 1958; van Lier et al., 1960; Tester et al., 1977; Rimstidt and Barnes, 1980; Robinson, 1982). The mass of water $M_w$ is calculated as the product of the reactor liquid volume and the density of the water at reaction conditions. The total quartz surface area $A_s$ is calculated by multiplying the specific surface area $a_s$ by the mass of quartz used $M_{qtz}$. A geometric surface area basis is used in this article as discussed in Tester et al. (1994). The CSTR assumption allows $r_{\text{net}}$ to be calculated directly from easily measured parameters

$$r_{\text{net}} = \left(m^{\text{out}}_{H_4SiO_4} - m^{\text{in}}_{H_4SiO_4}\right)/\tau \tag{2}$$

where $r_{\text{net}}$ is the net dissolution rate (mol/kg-s), $\tau$ is the nominal average residence time (s) of the reactor (liquid mass in the reactor divided by the mass-flow rate through the reactor), and $m^{\text{out}}_{H_4SiO_4}$ and $m^{\text{in}}_{H_4SiO_4}$ are the concentrations (mol/kg) of the outlet and inlet streams to the reactor, respectively. In our experiments, the inlet concentration is always equal to zero.

An estimate of $m^{\text{sat}}_{H_4SiO_4}$ is needed as a function of temperature and pressure in the two-component, binary mixture of quartz ($SiO_2$) and water ($H_2O$) in order to extract a rate constant for dissolution ($k_f$). In this study, we use the Fournier and Potter (1982) correlation for quartz solubility. Although this correlation fits a wide range of data very well, there may be some errors associated with its use, especially at low temperatures. Fortunately, the data in our study were obtained at concentrations much lower than the saturated value, therefore $k_f$ is not significantly affected by uncertainties in $m^{\text{sat}}_{H_4SiO_4}$.

## Ionic Speciation Calculation

The concentration of ions in solution must be calculated at the reaction temperature in order for correlations to be meaningful. Based on the quantities of acid, base, and/or salt added to the feed tank at room temperature and the room temperature pH, a model was developed to calculate the ion concentration in the reactor. This model uses an iterative procedure to solve the equilibrium relations and the charge balance, incorporating experimental dissociation constants published in literature with activity coefficients calculated from an extended Debye-Hückel equation (Zemaitis et al., 1986). The concentration of dissolved carbon dioxide is an important parameter. It was calculated using the speciation model based on the outlet pH of the reactor effluent which was cooled in a tube-in-tube heat exchanger to approximately 25°C before being exposed to air. The pH was measured quickly to minimize carbon dioxide uptake from air. The estimated carbon dioxide concentration was substituted into the speciation model to calculate the pH, pOH, and all the ionic concentrations. A complete description of the model is given in the Appendix.

## Correlation of pH and Ionic Strength Effects on Kinetics

Based on earlier experiments at low temperature in our laboratory and elsewhere (Gratz et al., 1990, 1993; Dove, 1994; Kamiya et al. (1974); Wollast and Chou, 1986; Brady and Walther, 1989, 1990), we adopt the basic hypothesis that $H^+$ and $OH^-$ catalyze the dissolution rate by some mechanism of interaction with the quartz surface. In all this previous work, with the exception of Gratz et al. (1990, 1993) and Dove (1994), rate data were reported as the logarithm of the net dissolution rate vs. pH. There are two potential complications with this approach. First, when correlating data over a range of temperatures at high pH, changes in the dissociation constant of water can affect the apparent activation energy. Second, the concentration of $H^+$ (or $OH^-$) may be a more appropriate regression parameter, rather than the activity. This issue is very difficult to resolve experimentally since dissolution rates can change rapidly with changes in solution composition, while the activity coefficients of dissolved species ($H_4SiO_4$, $Na^+$, etc.) may only change slightly. For these situations, activities and concentrations would most likely vary

similarly, and the quality of the regressions will be comparable regardless of which basis is used.

In the absence of any general mechanism or theory, the functional form of the relationship between the dissolution rate and the species concentrations is fit empirically using a global rate law format. Care must be taken not to extract mechanistic insights from such a global correlation. It merely provides a convenient way of representing the data.

At low pH there was little effect of $OH^-$ concentration on dissolution rate, and are therefore difficult to correlate in a statistically significant manner. As a first approximation, the rate data in neutral and basic solutions can be represented with a simple global rate law of the following form

$$k_f = k_{OH,Na} m_{OH^-}^b m_{Na^+}^c \tag{3}$$

where $k_f$ is the global dissolution rate constant, $m_{OH^-}$ and $m_{Na^+}$ are molalities of $OH^-$ and $Na^+$, $b$ and $c$ are the apparent reaction orders of $OH^-$ and $Na^+$, respectively, and $k_{OH,Na}$ is an empirical rate constant with the dependencies on $m_{OH^-}$ and $m_{Na^+}$ factored out of $k_f$. Although the form of the rate law in Eq. 3 can be traced to elementary reaction modeling where $b$ and $c$ are integers and represent the stoichiometries of the reactants involved in the activated complex, we are using it to model complex kinetics more globally with several elementary reactions involved. In this case, $b$ and $c$ are fitted to the experimental data and are no longer constrained to be integers. In this context, as fitted parameters they convey no mechanistic information at a molecular level. Parameters regressed from experimental data using Eq. 3 are only valid for the particular system studied. For example, parameters regressed from a NaOH/NaCl mixture will not necessarily equal those from a $NaOH/Na_2SO_4$ mixture.

## Results

The dissolution experiments carried out in order to quantify the effects of adding different electrolytes to the quartz-water system are described below.

### *Effect of $H^+$ with no salt present*

Two sets of experiments were carried out in the spinning basket reactor at 175°C and 200°C to evaluate the effect of $HNO_3$ on the dissolution rate of quartz (see Table 2 for run data). Figure 3 displays the results of these experiments on a log $k_f$ vs. pH (at 23°C) graph. The pH at the reaction temperature would be a more appropriate abscissa, however, the pH of $HNO_3$ solutions changes very little with temperature from 175° to 23°C, because it is a strong acid ( ~ 100% dissociated) and the mean ionic activity coefficient $\gamma_{\pm}$ ($HNO_3$) does not change much with temperature. The data at 175°C show a decreasing trend in $k_f$ as pH is lowered from pH 4 to pH 3. A relatively pH independent region exists from pH 3 to pH 1.5. At pH 1.1, the dissolution rate begins to increase. At 200°C, the data show a decreasing trend from pH 4 down to pH 2.3. The qualitative behavior at 175°C and 200°C is consistent with the previous work performed at 25 to 90°C (Kamiya et al., 1974; Kline and Fogler, 1981b; Wollast and Chou, 1986; Knauss and Wolery, 1988; Grigsby, 1989; Brady and Walther, 1990; House and Orr, 1992).

**Table 2. Experimental Data Investigating the Effect of $H^+$ (from $HNO_3$) on the Dissolution Rate of Ottawa Sand**

| Run No. | Spinning Rate rpm | Flow Rate $10^{-6}$ kg/s | $m_{H_4SiO_4}$ $10^{-6}$ mol/kg | log $k_f$ mol/m$^2$·s | pH at 23°C |
|---|---|---|---|---|---|
| *175°C* | | | | | |
| 70 | 190 | 178 | 11.0 | −8.95 | 1.58 |
| 71a | 180 | 1,402 | 1.5 | −8.93 | 1.58 |
| 71b | 180 | 656 | 2.7 | −8.99 | 1.58 |
| 72 | 190 | 239 | 5.6 | −9.12 | 2.29 |
| 74 | 180 | 302 | 5.2 | −9.05 | 2.83 |
| 76 | 180 | 136 | 28.5 | −8.65 | 3.45 |
| 78 | 180 | 302 | 11.1 | −8.72 | 3.98 |
| 80 | 190 | 975 | 3.3 | −8.73 | 1.10 |
| 81 | 155 | 367 | 3.7 | −9.11 | 1.54 |
| 82 | 155 | 238 | 5.5 | −9.13 | 1.85 |
| *200°C* | | | | | |
| 73 | 190 | 1,510 | 2.6 | −8.66 | 2.30 |
| 75 | 190 | 1,569 | 5.1 | −8.29 | 2.83 |
| 77 | 190 | 1,434 | 8.5 | −8.11 | 3.45 |
| 79 | 180 | 1,627 | 8.3 | −8.06 | 3.98 |

### *Effect of $OH^-$ (using NaOH)*

The results for experiments investigating the effect of $OH^-$ on the dissolution rate of Ottawa sand in NaOH solutions are plotted in Figure 4 (see Table 3 for run data). A remarkably linear fit to the data is obtained by plotting the logarithm of the dissolution rate constant $k_f$ vs. the logarithm of the hydroxide ion concentration (estimated using the speciation model discussed in the Appendix). The hydroxide ion concentrations in Figure 4 are derived from deionized water to 0.01 molal NaOH solutions.

The slopes or apparent reaction orders for hydroxide ion, shown in Figure 4, varied from 0.72 (±0.14) at 100°C to 0.88 (±0.04) at 200°C (please note that all ± ranges given in this article are at 95% confidence limits). Thus, an empirical equation of the form

$$k_f = k_{OH} m_{OH^-}^{b'} \tag{4}$$

is adequate to describe quartz dissolution rate data in NaOH solutions, where $k_{OH}$ is an empirical dissolution rate constant $m_{OH^-}$ is the molality of $OH^-$ in solution, and $b'$ is the apparent reaction order on $OH^-$ with the effect of $Na^+$ em-

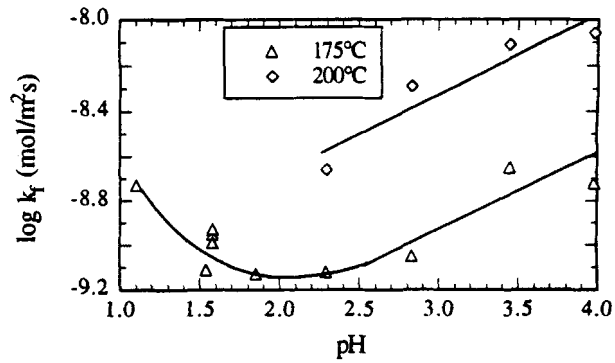


**Figure 3. Quartz dissolution results in low pH at 23°C solutions of $HNO_3$ at 175°C and 200°C.**
Lines drawn to illustrate trends only.

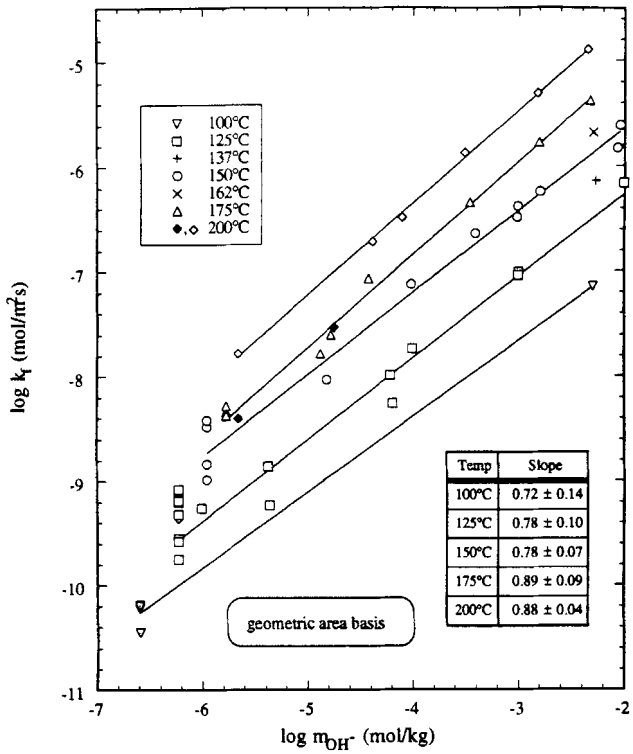


**Figure 4. Quartz dissolution: effect of added NaOH with no salts present.**

Two-parameter linear regression results shown (95% confidence). Note that two outlier points (F) at 200°C were omitted from the regression and the average of the deionized water runs was used in the regression.

bedded in it. All of the data plotted in Figure 4 are included in the regressions except for two points (one deionized water run and one run at log $m_{OH^-} = -4.8$) at 200°C that are clearly outliers (shown as filled in diamonds), lying 0.6 log units below the regressed line. These omitted runs (126 and 127) were performed sequentially, but no explanation can be given for their wide deviation from the other data at 200°C.

Equation 4 incorporates the effect of $Na^+$ into the value of $b'$. Thus, we would like to decouple the effects of $Na^+$ from the effects of $OH^-$. A multivariate linear regression of these data using Eq. 3 would result in inaccurate values of $b$ and $c$. Therefore, experiments were carried out at constant $Na^+$ (using NaCl) and variable $OH^-$, and at constant $OH^-$ and variable $Na^+$, to more rigorously validate the correlation and the regression parameters in Eq. 3.

### *Effect of $OH^-$ at constant $Na^+$*

Experiments were performed at 150°C to investigate the effect of $OH^-$ on the dissolution rate of quartz at a constant $Na^+$ (0.01 molal) to decouple the effect of $OH^-$ from the effect of $Na^+$ in solution (see Table 4 for run data). Solutions varied from a 0.01 molal NaCl solution to 0.01 molal NaOH solution. The results are plotted in Figure 5 using log $[k_f/(m_{Na^+})^c]$ vs. log $m_{OH^-}$ coordinates to account for any variation in $Na^+$ between experiments and to allow calculation of $b$ in Eq. 3 by a simple linear regression which represents the data well. The value of $c$ is arbitrary, however, since $m_{Na^+}$ is approximately constant, identical results were obtained for $c = 0.2$ to 0.4. Figure 5 shows that $b = 0.58\ (\pm 0.17)$ to 95% confidence assuming $c = 0.3$.

Although these results are only strictly valid for 150°C and $m_{Na^+} = 0.01$ molal, the studies shown in Figure 4 suggest that the combined effect of $Na^+$ and $OH^-$ does not change measurably from deionized water to 0.01 molal NaOH solutions. Therefore, $b$ and $c$ are not expected to be strongly concentration dependent in the range of concentrations shown in Figure 4 (up to 0.01 molal). The value of $b$ may change with temperature since the slopes in Figure 4 appear to be slightly temperature-dependent, but given the scatter in the data we cannot claim a high degree of statistical significance to this dependence.

### *Effect of $Na^+$ at constant $OH^-$*

The results of the experiments investigating the effect of $Na^+$ ranging from $1 \times 10^{-3}$ to 1.25 molal on $k_f$ at 150°C with a constant $OH^-$ concentration of approximately $10^{-3}$ molal in NaOH/NaCl solutions are shown in Figure 6 using Eq. 3 as the basis for the correlation (see Table 5 for run data). Linear regressions on a log $[k_f/(m_{OH^-})^b]$ vs. log $m_{Na^+}$ result

**Table 3. Experimental Data Investigating the Effect of $OH^-$ (from NaOH) on the Dissolution Rate of Ottawa Sand Shown in Figure 4**

| Run No. | Spinning Rate rpm | Flow Rate $10^{-6}$ kg/s | $m_{H_4SiO_4}$ $10^{-6}$ mol/kg | log $k_f$ mol/m²·s | log $m_{OH^-}$ at $T$ mol/kg | log $I$ at $T$ mol/kg |
|---|---|---|---|---|---|---|
| *100°C* | | | | | | |
| 6 | 140 | 15.0 | 8.27 | −10.19 | −6.60 | −5.65 |
| 8 | 200 | 12.3 | 9.32 | −10.22 | −6.60 | −5.65 |
| 17 | 112 | 15.5 | 7.90 | −10.2 | −6.60 | −5.65 |
| 47 | 110 | 32.6 | 1.75 | −10.45 | −6.60 | −5.65 |
| 134 | 320 | 246 | 78.9 | −7.15 | −2.29 | −2.25 |
| *125°C* | | | | | | |
| 3–5 | 15–85 | 153 | 5.99 | −9.32 | −6.22 | −5.68 |
| 10 | 105 | 162 | 7.35 | −9.2 | −6.22 | −5.68 |
| 12 | 90 | 154 | 10.4 | −9.08 | −6.22 | −5.68 |
| 27 | 110 | 69.8 | 18.3 | −9.17 | −6.22 | −5.68 |
| 37 | 110 | 84.7 | 12.3 | −9.19 | −6.22 | −5.68 |
| 43 | 110 | 66.5 | 6.82 | −9.55 | −6.22 | −5.68 |
| 53 | 110 | 78.4 | 3.63 | −9.75 | −6.22 | −5.68 |
| 54 | 110 | 66.5 | 6.36 | −9.58 | −6.22 | −5.68 |
| 90 | 120–205 | 371 | 74.9 | −7.73 | −4.00 | −3.92 |
| 92 | 90 | 390 | 2.25 | −9.26 | −6.01 | −5.46 |
| 97 | 195 | 269 | 58.1 | −7.99 | −4.21 | −3.89 |
| 99 | 112 | 607 | 3.93 | −8.86 | −5.37 | −4.92 |
| 100 | 107 | 593 | 15.9 | −8.26 | −4.19 | −3.74 |
| 101 | 107 | 191 | 5.24 | −9.23 | −5.36 | −4.82 |
| 103 | 220 | 3,199 | 51.9 | −7.01 | −3.00 | −2.96 |
| 104 | 110 | 256 | 32.4 | −7.04 | −3.00 | −2.94 |
| 106 | 220 | 1,507 | 42.3 | −6.16 | −2.01 | −1.99 |
| *137°C* | | | | | | |
| 133 | 320 | 857 | 223 | −6.14 | −2.27 | −2.25 |
| *150°C* | | | | | | |
| 9 | 105 | 282 | 22.0 | −8.48 | −5.95 | −5.67 |
| 11 | 230 | 389 | 18.7 | −8.42 | −5.95 | −5.67 |
| 93 | 230 | 377 | 3.61 | −8.99 | −5.95 | −5.67 |
| 98 | 210 | 216 | 11.6 | −8.84 | −5.95 | −5.67 |
| 124 | 128 | 206 | 11.6 | −8.03 | −4.82 | −4.61 |
| 91 | 87 | 2,095 | 56.4 | −7.12 | −4.01 | −3.92 |
| 105 | 110 | 1,587 | 24.4 | −6.38 | −3.01 | −2.94 |

**Table 3. Experimental Data Investigating the Effect of $OH^-$ (from NaOH) on the Dissolution Rate of Ottawa Sand Shown in Figure 4. Continued**

| Run No. | Flow Rate ($10^{-6}$ kg/s) | $m_{H_4SiO_4}$ ($10^{-6}$ mol/kg) | log $k_f$ (mol/m$^2$s) | log $m_{OH^-}$ at T (mol/kg) | log $I$ at T (mol/kg) |
|---|---|---|---|---|---|
| *150°C* | | | | | |
| 123 | 334 | 424 | −6.24 | −2.80 | −2.70 |
| 89 | 2,001 | 1,747 | −5.61 | −2.04 | −1.92 |
| 136 | 440 | 135 | −6.64 | −3.41 | −3.35 |
| 151 | 467 | 181 | −6.48 | −3.01 | −2.94 |
| 152 | 783 | 508 | −5.83 | −2.07 | −2.00 |
| *162°C* | | | | | |
| 135 | 1,552 | 35.3 | −5.68 | −2.29 | −2.25 |
| *175°C* | | | | | |
| 62 | 530 | 13.6 | −8.38 | −5.77 | −5.64 |
| 63 | 881 | 9.07 | −8.34 | −5.77 | −5.64 |
| 64 | 937 | 7.80 | −8.38 | −5.77 | −5.64 |
| 67 | 924 | 10.0 | −8.28 | −5.77 | −5.64 |
| 85 | 362 | 22.9 | −8.28 | −5.77 | −5.64 |
| 87 | 321 | 21.1 | −8.37 | −5.77 | −5.64 |
| 118 | 269 | 16.8 | −7.78 | −4.87 | −4.68 |
| 121 | 415 | 280 | −6.34 | −3.46 | −3.39 |
| 122 | 588 | 689 | −5.77 | −2.80 | −2.70 |
| 125 | 201 | 34.0 | −7.6 | −4.77 | −4.61 |
| 137 | 221 | 103 | −7.07 | −4.41 | −4.33 |
| 138 | 1,421 | 745 | −5.38 | −2.33 | −2.25 |
| *200°C* | | | | | |
| 65 | 2,017 | 11.5 | −7.88 | −5.66 | −5.60 |
| 66 | 1,682 | 15.7 | −7.82 | −5.66 | −5.60 |
| 86 | 2,185 | 16.8 | −7.63 | −5.66 | −5.60 |
| 126* | 216 | 4.99 | −8.40 | −5.66 | −5.60 |
| 127* | 186 | 43.3 | −7.53 | −4.74 | −4.61 |
| 128 | 437 | 717 | −5.87 | −3.50 | −3.42 |
| 129 | 450 | 196 | −6.48 | −4.10 | −4.05 |
| 130 | 1,537 | 765 | −5.31 | −2.82 | −2.74 |
| 131 | 474 | 110 | −6.71 | −4.37 | −4.28 |
| 132 | 2,247 | 1,354 | −4.90 | −2.35 | −2.25 |

*Omitted from regression

in a slope of 0.25 (±0.10) for $b = 0.58$. Identical results were obtained for $b = 0.48$ to 0.68. Clearly, the assumed value of $b$ is not critical in the analysis of rate data at approximately constant $m_{OH^-}$. The effect of $Na^+$ appears to be leveling off above log $m_{Na^+} = -0.9$ ($m_{Na^+} = 0.13$ molal). The slope of the regression was 0.31 (±0.06), neglecting the two high $m_{Na^+}$ points.

Experiments were also performed using $Na_2SO_4$ to vary the $Na^+$ concentration instead of NaCl to investigate for the possible effects of the chloride anion. Results of these experiments are shown in Figure 6. The log $m_{Na^+} = -2.0$ point agrees well with the NaCl point at the same concentration. However, further increases in $Na^+$ concentration do not result in an experimentally significant increase in the rate. It appears that at the same molal concentration NaCl accelerates dissolution more than $Na_2SO_4$. This could imply an enhancing effect of $Cl^-$ and/or an inhibiting effect of $SO_4^=$ (or $HSO_4^-$). Perhaps, $SO_4$ = ions adsorb on the quartz surface limiting the effectiveness of attack by $OH^-$ and $Na^+$, however, as there are no known silica sulfate minerals, the absorption will likely be physical rather than chemical. The effect of the anion adsorption is expected to be small, since at these concentrations of $OH^-$ the quartz surface is negatively charged, which should hinder the adsorption of the negatively charged anion.

**Table 4. Experimental Data Investigating the Effect of $OH^-$ at Constant $Na^+$ Shown in Figure 5**

| Run No. | Flow Rate $10^{-6}$ kg/s | $m_{H_4SiO_4}$ $10^{-6}$ mol/kg | log $k_f$ mol/m$^2$·s | log $m_{OH^-}$ at 150°C mol/kg | log $I$ at 150°C mol/kg |
|---|---|---|---|---|---|
| 141 | 179 | 17.5 | −7.94 | −5.797 | −2.000 |
| 140 | 371 | 151 | −6.66 | −4.114 | −2.000 |
| 139 | 628 | 57.6 | −6.14 | −3.075 | −2.000 |
| 89 | 2,077 | 1,747 | −5.61 | −2.042 | −1.924 |
| 152 | 783 | 508 | −5.83 | −2.066 | −1.998 |

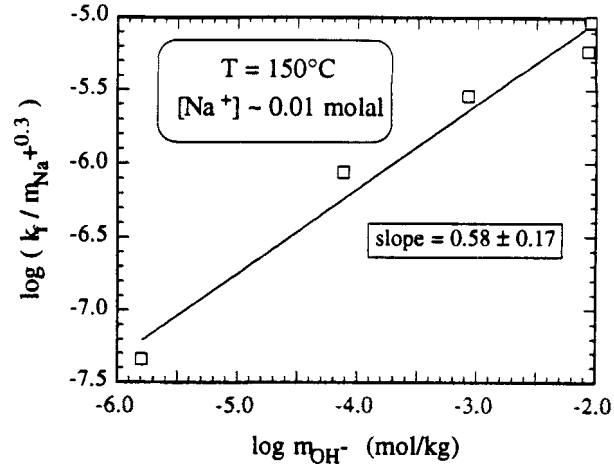


**Figure 5. Quartz dissolution showing effect of $OH^-$ at constant $Na^+$ (~ 0.01 molal).**
See Table 4 for the data.

As pointed out in the description of the ionic speciation model in the Appendix, NaCl and $Na_2SO_4$ were assumed to be completely dissociated, which should be a good assumption for the conditions in this study.

Despite the differences between the NaCl and $Na_2SO_4$ experimental results, both data sets display a leveling off of the

**Table 5. Experimental Data Investigating the Effect of $Na^+$ (from NaCl) on the Ottawa Sand Dissolution Rate at Constant $OH^-$ and $T = 150$°C Shown in Figure 6**

| Run No. | Flow Rate $10^{-6}$ kg/s | $m_{H_4SiO_4}$ $10^{-6}$ mol/kg | log $k_f$ (mol/m$^2$·s) | log $m_{OH^-}$ at 150°C mol/kg | log $I$ at 150°C mol/kg |
|---|---|---|---|---|---|
| *NaCl* | | | | | |
| 105 | 1,587 | 24.5 | −6.38 | −3.005 | −2.943 |
| 139 | 628 | 288 | −6.14 | −3.075 | −2.000 |
| 148 | 585 | 290 | −6.17 | −3.075 | −2.000 |
| 142 | 638 | 429 | −5.93 | −3.065 | −1.230 |
| 143 | 779 | 418 | −5.83 | −3.077 | −0.850 |
| 149 | 1,402 | 281 | −5.79 | −3.134 | 0.097 |
| 151 | 467 | 181 | −6.48 | −3.011 | −2.944 |
| 153 | 887 | 253 | −5.80 | −3.091 | −0.347 |
| *$Na_2SO_4$* | | | | | |
| 105 | 1,587 | 24.5 | −6.38 | −3.005 | −2.943 |
| 146 | 419 | 388 | −6.17 | −3.024 | −2.028 |
| 145 | 728 | 368 | −5.96 | −2.956 | −1.017 |
| 150 | 871 | 275 | −6.02 | −2.96 | −0.154 |
| 151 | 467 | 181 | −6.48 | −3.011 | −2.944 |
| 154 | 690 | 253 | −6.16 | −2.951 | −0.631 |

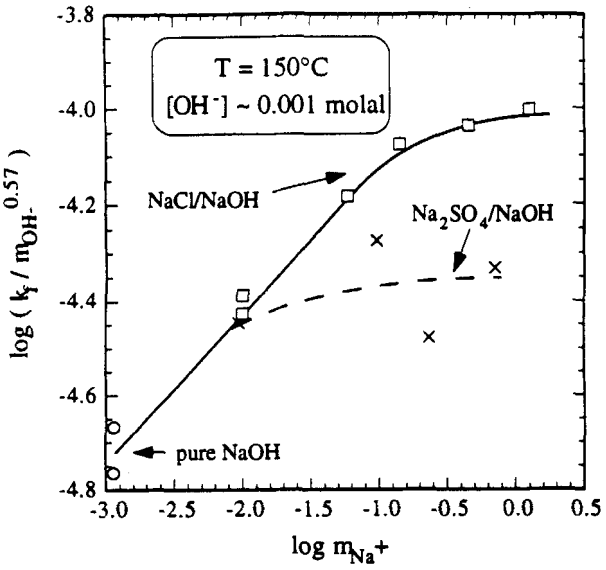


**Figure 6. Quartz dissolution results at 150°C showing effect of $Na^+$ ($Na_2SO_4$ vs. NaCl) at constant $OH^-$ (~0.001 molal).**

Lines drawn to indicate trends only.

$Na^+$ enhancement effect. This behavior is consistent with a concentration saturation effect on the quartz surface with respect to the salt added.

### *Regression analysis of dissolution rate data*

The individual regression analyses in previous two sections could have been replaced by a single multivariate analyses, however, simple graphs like Figures 5 and 6 could not have been drawn to visually validate the goodness of fit. In this section, a multivariate analyses is employed to estimate the parameters in Eq. 3, using the NaOH/NaCl data in the present study at 150°C. The two high $m_{Na^+}$ runs were excluded from the analysis, since these data showed that the dissolution rate levels off as $m_{Na^+}$ is increased and the global kinetic model given in Eq. 3 cannot predict this behavior.

Equation 3 was useful in fitting most of our rate data, however, it cannot be used to estimate the dissolution rates in deionized water. Since Figure 4 showed that the experiments in NaOH solutions only extrapolated well to the deionized water data, we would like to derive a single relationship that can describe all of our data, including experiments in deionized water and NaOH/NaCl solutions. The following simple equation was found to be effective in correlating our rate data

$$k_f = k_{OH,I} m_{OH^-}^b I^c \tag{5}$$

where $I$ is the ionic strength of the solution in units of molality and $k_{OH,I}$ is the empirical rate constant used to factor out the dependencies on $m_{OH^-}$ and $I$ from $k_f$. The ionic strength is defined by

$$I = \frac{1}{2} \sum_i z_i^2 m_i \tag{6}$$

where $z_i$ and $m_i$ are the ionic charge and molality (mol/kg $H_2O$) of each cationic and anionic species $i$, respectively. The value of $I$ is essentially equivalent to $m_{Na^+}$ for all solutions except for the deionized water runs where it is equivalent to $m_{H^+}$. The choice of $I$ was used for calculational convenience to capture the effects of increasing salinity. It does not suggest that the apparent reaction order $c$ will be the same for any salt at the same ionic strength. The apparent reaction order of $I$ in Eq. 5 is called $c$ since it conveys essentially the same information as $c$ in Eq. 3 for NaOH/NaCl solutions.

To linearize the power law form of the rate law, the logarithm of Eq. 5 is taken

$$\log k_f = \log k_{OH,I} + b \log m_{OH^-} + c \log I \tag{7}$$

Regressed values of $b$ and $c$ are expected to be similar to those found earlier with minor adjustments made for the inclusion of the pure NaOH and deionized water runs. Using the Powell regression technique (Kuester and Mize, 1973), $b$ and $c$ were calculated to be 0.57 (±0.07) and 0.26 (±0.06), respectively. The goodness of fit can be evaluated by plotting the modeled $k_f$ vs. the experimental $k_f$. Based on the fit in Figure 7, Eq. 5 represents the data well for $m_{OH^-}$ from $3 \times 10^{-7}$ to 0.01 molal and $m_{Na^+}$ from 0 to 0.1 molal.

We would like to calculate $b$ and $c$ from 125 to 200°C. Unfortunately, since these data investigated the effect of added NaOH only, decoupling the effects of $OH^-$ and $Na^+$ is difficult. The value of $c$ has not been well characterized and no obvious trends exist as a function of temperature. For this study, if we assume $c$ equals 0.26 from 100 to 200°C and for $m_{Na^+}$ less than 0.1 molal in NaOH/NaCl solutions, then we can estimate $b$ from a linear regression of the data in Figure 4, by correlating $\log [k_f/I^c]$ vs. $\log m_{OH^-}$. The resulting slopes or $b$ values are compared to results from previous studies in Figure 8—note that apparent reaction orders from

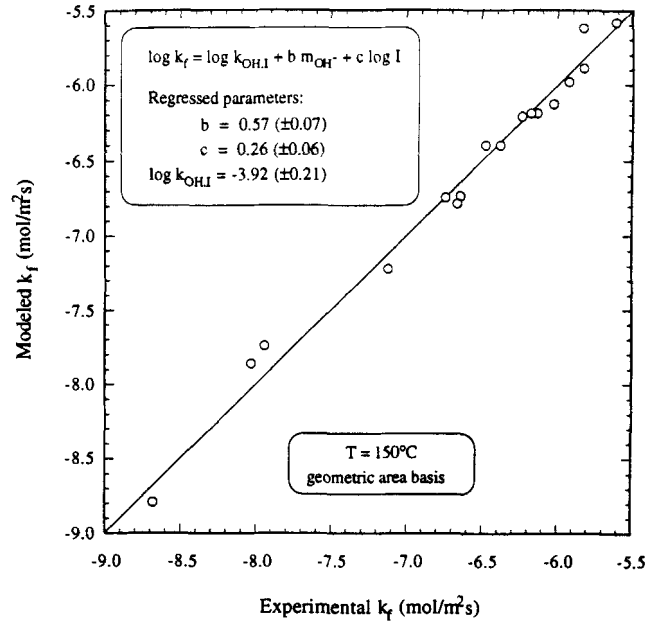


**Figure 7. Modeled log $k_f$ plotted against experimental log $k_f$ at 150°C (this study).**

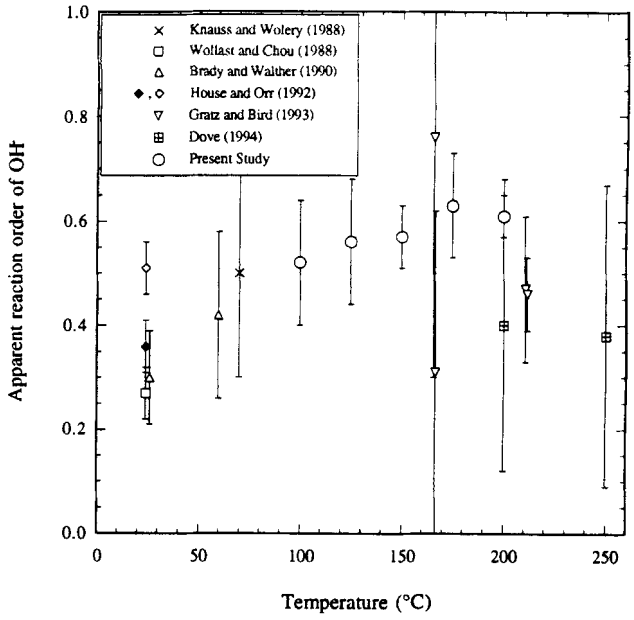


**Figure 8. Apparent reaction order *b* of $OH^-$ as a function of temperature.**

See text for discussion of House and Orr (1993) data point.

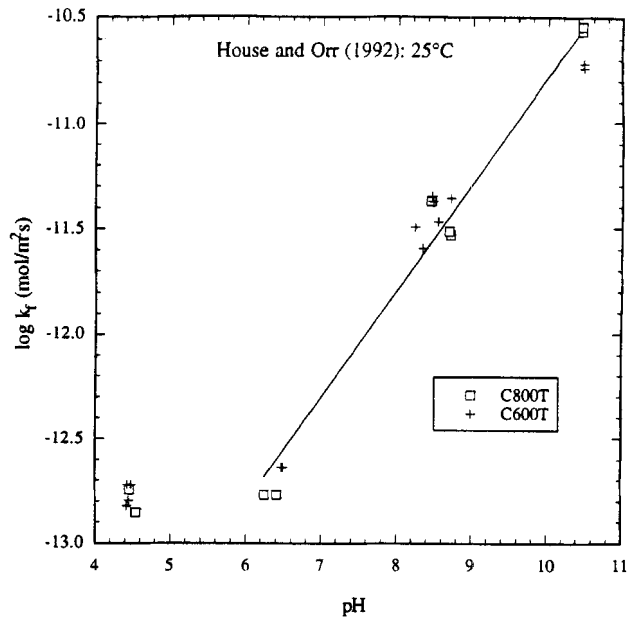


**Figure 9. Dissolution rate constants from House and Orr (1992) study investigating the pH dependence of quartz dissolution.**

this study are higher than those derived from previous researchers at lower temperatures. These values in general were not reported in the original papers; therefore, we analyzed the published results and the assumptions made in these calculations must be clearly presented here. For example, House and Orr (1992) investigated the pH dependence of quartz dissolution and found $b = 0.36$ (filled-in symbol). However, they included the pH ~ 4.45 data points in their analysis. At this pH, quartz dissolution is nearly independent of pH and we believe that these low pH ( ~ 4.45) data points should not be used. Their data are shown in Figure 9. Neglecting the data at low pH yields a $b$ value of 0.51 (open symbol) which is higher than the results of Brady and Walther (1990) and Wollast and Chou (1986). We are trying to analyze the linear region which at 25°C is typically observed from pH 7 to pH 12. Higher concentrations of hydroxide ion have not been frequently studied. The data of Gratz and coworkers (1990, 1993) suggest that at high concentration, the effect of OH levels off. A similar conclusion was reached by Dove and Elson (1992). Data from Gratz and Bird (1993) at 211°C and I = 0.01 molal are shown in Figure 10. We chose to neglect two points in the rhombohedron face and one point on the prism face. Although, the selection of points to omit is somewhat arbitrary, we wanted to eliminate the plateau frequently seen at high $OH^-$ in the data of Gratz and coworkers (1990, 1993).

Initially, when we looked at only our own data taken at lower temperatures, we thought that $b$ increased with temperature. However, with the more recent higher-temperature studies by Gratz and coworkers (1990, 1993), Berger et al. (1994), and Dove (1994), this hypothesis is questionable. In order to model our data from 100 to 200°C, we have chosen to assume $b$ is constant with temperature in this range and equal to the average of $b$ values found by us and others between 100 and 211°C. However, due to the large uncertainties in the Gratz and Bird (1993) data at 166°C, we have neglected these data in our average. The resulting average is $b = 0.53$.

The large error bars for some of the data is due to small number of points used in the regressions. We have used 95% confidence limits to define the error bars. Thus the standard error estimate in the regression is multiplied by the appropriate t-value, which can be rather high at low degrees of freedom.

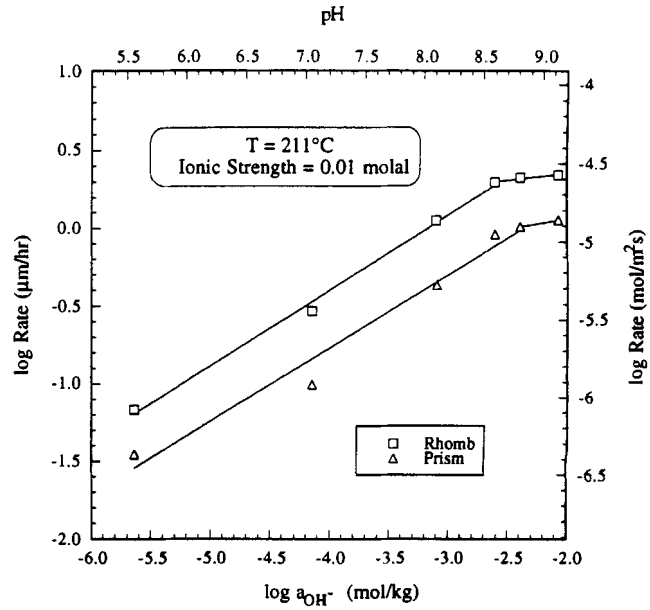


**Figure 10. Dissolution rate constants from Gratz and Bird (1993) study investigating the $OH^-$ dependence of quartz dissolution.**

### *Activation energy for quartz dissolution*

Apparent global activation energies for quartz dissolution in deionized water have been reported by many investigators (Siebert et al., 1963; Rimstidt and Barnes, 1980; Brady and Walther, 1990; Dove and Crerar, 1990; Bennett, 1991; and others); however, very little is known about the activation energy in other environments. In deionized water, values range from 71 (±11) kJ/mol (Dove and Crerar, 1990) to 89 (±5) kJ/mol (Tester et al., 1994). In buffered solutions, Brady and Walther (1990) found that the activation energy between 25°C and 60°C was pH dependent, being 46 kJ/mol at near-neutral pH and increasing to 54 kJ/mol at pH 8 and 96 kJ/mol at pH 11. In a more recent and comprehensive study, Dove (1994) reports an elaborate set of data for 274 experimental conditions. Dove (1994) calculated the activation energy based upon fitting of experimental data from 25 to 300°C for solution $pH_T$ of 2 to 12 and 0 to 0.3 molal sodium using a surface reaction model. The resultant expression yielded activation energies of 68.5 (±2.3) and 85.2 (±2.1) on SiOH and $SiO^-$ sites, respectively. Although these results are in general agreement with previously published results, they should not be compared directly since a completely different model was used to derive the activation energy.

Obviously, from the above discussion, the basis for the activation energy calculation is very important. Since at near-neutral and higher pH, quartz dissolution is base-catalyzed, the activation energy should be calculated at constant $m_{OH^-}$ or constant pOH. All activation energies reported in this study are apparent activation energies, since little is known about the actual elementary reactions that govern quartz dissolution. Thus, the apparent global activation energy is model dependent. For example, if a rate law is proposed such that $k_f = k_{H_2O}\, m_{OH^-}$ in deionized water, then the apparent activation energy of $k_f$ will be different from the apparent activation energy in $k_{H_2O}$ since $m_{OH^-}$ in deionized water changes with temperature.

The simplest method for calculating the apparent activation energy is to track changes in $k_f$ at some defined set of constant conditions. This method is attractive since it involves only the overall dissolution rate (see Eq. 1) and makes no assumptions about the actual rate law for quartz dissolution. Unfortunately, it does not necessarily yield meaningful values for the activation energy of quartz dissolution. However, we will employ this method as a basis for comparison with the results of previous research. Based upon the least-squares regressions in Figure 4, values of $k_f$ at log $m_{OH^-}$ = −2.5, −4.0, and −5.5 were interpolated from 100 to 200°C and plotted on Arrhenius coordinates. The apparent activation energy (in kJ/mol) was found to be 60 (±12), 68(±7), and 77 (±2) for log $m_{OH^-}$ = −5.5, −4.0, and −2.5, respectively. These trends qualitatively support the results from Brady and Walther (1990) concerning the increase of the apparent activation energy of $k_f$ with increasing pH; however, the absolute magnitudes are higher than the values reported by Brady and Walther.

A more appropriate analysis of the apparent activation energy for quartz dissolution calculates the temperature dependence of $k_{OH,I}$ instead of $k_f$, since $k_{OH,I}$ factors the effects of solution composition out of $k_f$. Equation 5 is used to calculate $k_{OH,I}$ for the deionized water and all of the NaOH/NaCl data except the two highest NaCl runs. The value of $c$ is assumed to be 0.26, while $b$ is assumed to be 0.53. The calculated $k_{OH,I}$ values were plotted on Arrhenius coordinates resulting in an apparent activation energy of 72 (±6) kJ/mol, with the regression shown in Figure 11.

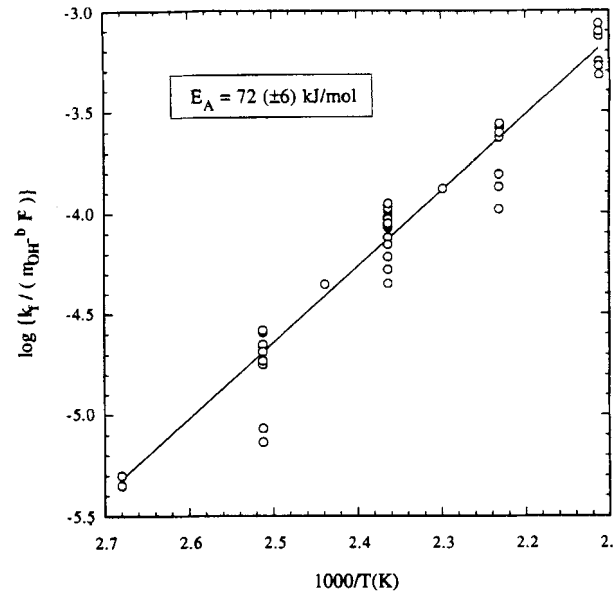


**Figure 11. Arrhenius plot of $k_{OH,I}$ from 100 to 200°C in NaOH/NaCl solutions assuming b = 0.53 and c = 0.26.**

### *Effect of quartz type/surface area basis*

Tester et al. (1994) showed that the geometric surface area basis was as good as the BET surface area basis for normalizing dissolution rate data in deionized water. This conclusion was based on data from different researchers using different experimental procedures. A check on this hypothesis was carried out in our experiments by studying the effect of $m_{OH^-}$ on the dissolution rate of crushed quartz crystals from Hot Spring, Arkansas (AR) at 150°C. Figure 12 shows a comparison of dissolution rates of Hot Springs, AR crystals to Ottawa sand on a geometric surface area basis. Considering the different surface morphology of the two types of quartz and the inherent uncertainty in the dissolution rates, very good agreement is obtained. It appears that at high $m_{OH^-}$, the Ottawa sand rates were only slightly slower than the Hot Springs, AR rates. The agreement would be somewhat poorer if a BET surface area basis was used, since roughness factors (ratio of BET surface area to geometric surface area) are higher for Ottawa sand (7.0) than for Hot Springs, AR crystals (5.5). The net effect of using a BET area basis rather than a geometric basis would be to decrease $k_f$ by 0.11 log units for Ottawa sand relative to Hot Springs, AR crystals. A linear least-squares fit to each data set results in slopes (or $b'$ values) of 0.78 (±0.07 and 0.91 (±0.07) for Ottawa sand and Hot Springs, AR crystals, respectively.

The results in this study and in Tester et al. (1994) showing that a geometric surface area basis outperforms the BET surface area basis may be somewhat controversial. Certainly, the geometric surface area measurement/calculation technique is rather crude. While the BET method captures the surface

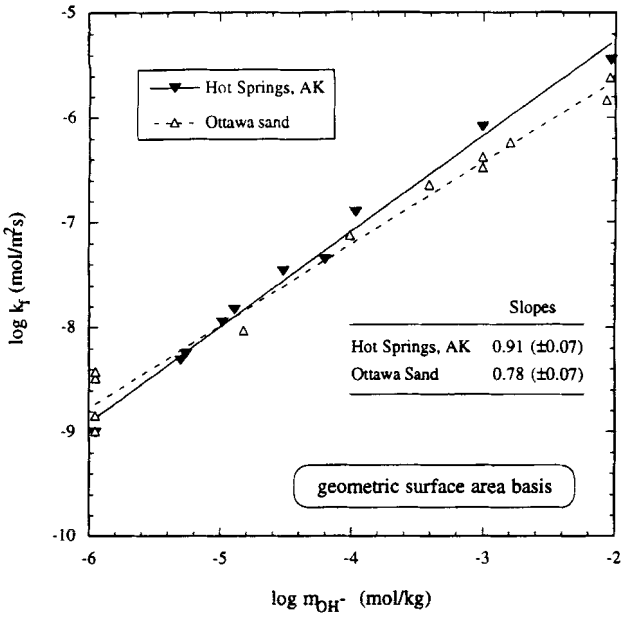


**Figure 12. Dissolution rates of Ottawa sand and Hot Springs, AR crystals in NaOH solutions at 150°C.**

area derived from the microtopography of the mineral sample, the true reactive surface area may be different from the BET value. For regression purposes, one needs a measurement technique which measures areas that are linearly proportional to the reactive surface area, while knowing its true value is not necessary.

## Composition Dependence Using Adsorption Models

The classical approaches to modeling quartz dissolution kinetics have employed empirical rate laws similar to those presented in this article by presenting data on log rate vs. pH coordinates (Knauss and Wolery, 1988; Grigsby, 1989; Brady and Walther, 1990; Bennett, 1991). A shortcoming of the fractional order empirical rate laws is that they were not based on any mechanistic information and the implied form of the rate data breaks down at high concentrations, suggesting a saturation of the quartz surface. The fractional rate laws have been rationalized using several arguments. Helgeson et al. (1984) proposed that the fractional orders result from fractional stoichiometries of species in the transition state complex. Lasaga (1981) explained the fractional orders based on the existence of a variety of surface sites with different adsorption and reaction energetics. A more likely explanation is that fractional orders are obtained since regressions are based on solution composition instead of surface composition. Several previous studies at 25°C have related the quartz dissolution rate to the surface charge, a measure of the $H^+$ or $OH^-$ adsorbed on the surface (Wirth and Gieskes, 1979; Fleming, 1986; Stumm et al., 1985; Blum and Lasaga, 1988; Brady and Walther, 1989, 1990).

Brady and Walther (1989) found that their quartz dissolution rates were first order with respect to the silica surface charge data ($\sigma$) of Bolt (1957) from pH 8 to 12 at 25°C. However, the surface charge of quartz and silica has been measured by many researchers using different particle types and different ionic strength adjusters. Gratz and Bird (1993) present a summary of these measurements, showing the variability of the results. Thus, Brady and Walther's choice of using Bolt's data is somewhat arbitrary. There is too much scatter in both the surface charge data and the dissolution rate data to conclusively state that the dissolution rate of quartz is first order with respect to surface charge.

Surface charge data at higher temperatures are required to perform a similar analysis on the high-temperature dissolution rate data performed in this study and others. Only two studies (Kita et al., 1981; Brady, 1992) of silica surface charge have been carried out at temperatures greater than 25°C. Kita et al. (1981) measured the surface charge of silica precipitated from $(C_2H_5O)_4Si$ at 40°C. Brady (1992) measured the surface charge of amorphous silica (200 m$^2$/g) at 60°C. However, more data are needed to understand the surface charge behavior of silica at temperatures above 25°C.

A second strategy to relate high-temperature dissolution rate data to surface charge would be to extend surface charge predictions based on various electrostatic models to higher temperatures. Although these models are very capable of representing data at 25°C, their validity at higher temperatures cannot be confirmed until accurate high-temperature surface charges are measured. The robustness of these models has been questioned in the literature (Sposito, 1983; Westall and Hohl, 1980). Westall and Hohl (1980) studied five electrostatic models and found that all models represent the data equally well, but the corresponding parameters in different models are not the same. They conclude that although the models are of the correct mathematical form to fit experimental data, they do not necessarily provide an accurate physical description of the interface.

Dove (1994) used the triple layer model of the interface (see Hayes and Leckie, 1987) to determine surface site distributions. Dove (1994) selected capacitances and surface site densities determined from low-temperature measurements and assumed they were constant to model high-temperature data. Dove also assumed the relative magnitudes of the surface association constants were independent of temperature, but she did assume that rate constants were covariant with $pK_w$ for water. Although this approach proved to be an effective tool to fit a wide range of data, her assumptions were not independently validated. To do this would require a very detailed set of additional experiments beyond the scope of the work reported.

Due to limitations in extrapolating electrostatic models to higher temperatures, classical adsorption isotherms (Langmuir and Freundlich) were used to fit our high-temperature data. These isotherms (discussed in the next two sections) are based on theoretical principles, but in our application, they will simply be used as empirical tools to further investigate the origin of fractional order kinetics and the saturation effect sometimes seen at high concentrations.

Langmuir and Freundlich isotherms originated from work in the area of heterogeneous catalysis. We will transform these relationships to apply to the adsorption of solution species onto the quartz surface, by replacing the partial pressure of gas A, $P_A$, with the concentration (molality) of species A in solution $m_A$. Once an expression for the fraction of quartz surface occupied by species A, $\theta_A$, on the quartz sur-

face is developed, a rate law may be established. As an initial assumption we will assume that the rate data can be described using the following rate equation

$$k_f = k_{\theta_A}\,\theta_A^n \tag{8}$$

Until more information is acquired, the first-order equation ($n = 1$) is the simplest and the most probable rate law for quartz dissolution. Orders higher than two would be hard to justify applying mechanistic analysis of elementary reaction steps. The goal of this rate law is to provide an explanation for fractional order kinetics and to model the saturation effect that is sometimes seen at high concentrations. If fractional orders are regressed solely from experimental data, then this rate equation is no more theoretically justified than the empirical rate law based on solution composition.

### *Langmuir isotherm*

The Langmuir isotherm is commonly used in catalytic studies due to its elegant simplicity and its usefulness as a building block for many kinetic expressions. Three important conditions are implied in the kinetic and statistical derivations of the Langmuir isotherm:

(1) Adsorption is localized and takes place only through collision of gas molecules (or solution species) with vacant sites.

(2) Each site can accommodate only one adsorbed species.

(3) The energy of an adsorbed species is the same at any site on the surface, and is independent of the presence or absence of nearby adsorbed species.

The Langmuir isotherm can be derived based on these assumptions using a kinetic approach (Satterfield, 1980), resulting in the following expression for a single vapor species A that adsorbs without dissociation, altered to represent the adsorption of species from a liquid solution

$$\theta_A = \frac{K_A^* m_A}{1 + K_A^* m_A} \tag{9}$$

where $K_A^*$ is the adsorption equilibrium constant for species A, $\theta_A$ is the occupied fraction of sites on which adsorption is possible, and $m_A$ is the molality of species A. Other expressions similar to Eq. 9 can be derived for more complicated adsorption situations (Satterfield, 1980).

Although the Langmuir isotherm can be derived from first principles both statistically and kinetically, the assumptions used in its derivation are seldom valid for a wide range of conditions. For instance, the heat of adsorption generally decreases with increasing coverage. Nonetheless, the Langmuir isotherm has proven to be a valuable empirical tool in the correlation of kinetic rate data.

Applying Eq. 9 to the first-order form ($n = 1$) of Eq. 8 yields the following rate equation

$$k_f = k_{\theta_A} \frac{K_A^* m_A}{1 + K_A^* m_A} \tag{10}$$

We will apply this equation to the two case studies performed at 150°C: (1) vary $m_{Na^+}$ at constant $m_{OH^-}$; (2) vary

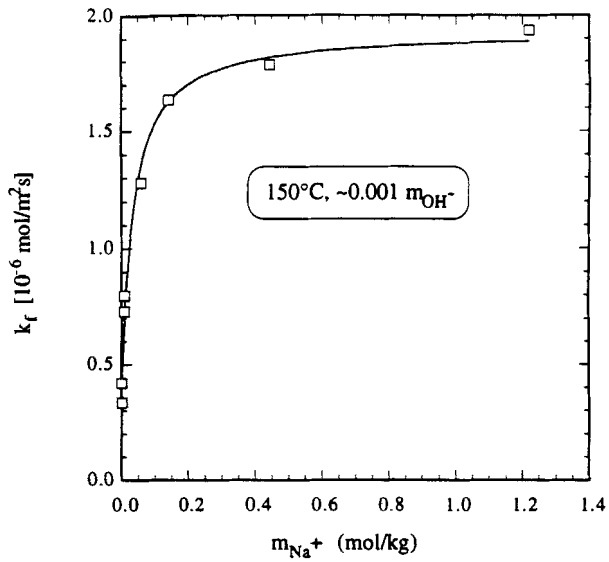


**Figure 13. Langmuir fit of the effect of $Na^+$ (NaCl) on 150°C quartz dissolution rates at constant $OH^-$ (this study).**

$m_{OH^-}$ at constant $m_{Na^+}$. The fractional order fit of case (1) varying $m_{Na^+}$ using NaCl cannot model the apparent saturation effect at high $m_{Na^+}$. A Langmuir fit of the model is shown in Figure 13, allowing for a nonzero dissolution rate at $m_{Na^+} = 0$. The intercept has no physical meaning in our system, since $m_{Na^+}$ cannot be zero because NaOH is used to maintain $m_{OH^-} = 1 \times 10^{-3}$ molal. The Langmuir model fits the rate data well, resulting in an adsorption equilibrium constant for $Na^+$, $K_{Na^+}^*$, of 30 ($\pm 14$) kg/mol at 150°C and $m_{OH^-} = 1 \times 10^{-3}$ molal. A similar analysis of the Dove and Crerar (1990) 200°C rate data for quartz dissolution in deionized water with varying amounts of added NaCl is shown in Figure 14. Although there is more uncertainty, a similar value of $K_{Na^+}^*$, 37 ($\pm 35$) kg/mol, was obtained. Dove and Crerar (1990) reported a different value for $K_{Na^+}^*$ because they calculated $K_{Na^+}^*$ by plotting $1/k_f$ vs. $1/m_{Na^+}$, and extracting $K_{Na^+}^*$ from the slope and intercept of regressed line. However, for comparison purposes we used the nonlinear form of Eq. 10 for both our data and Dove and Crerar's (1990) data.

The data shown in Figure 5 at constant $m_{Na^+}$ do not show a pronounced saturation effect with increasing $m_{OH^-}$; therefore, the fractional order model will be equally effective. The fit of these data using the Langmuir model is shown in Figure 15. Unfortunately, the scatter in the rate data, particularly at $m_{OH^-} > 0.008$ molal is too large to validate either model.

The Langmuir isotherm is very useful for modeling a saturation effect. It also makes use of a first-order model (Eq. 8), which provides an explanation of fractional order kinetics using very simplistic reasoning of adsorption phenomena on the quartz surface. The effectiveness of the Langmuir model, however, does not unequivocally prove that adsorption of $Na^+$ or $OH^-$ occurs on the quartz surface in such a fashion on a molecular level.

### *Freundlich isotherm*

It has been widely recognized that many systems do not obey the Langmuir isotherm. A popular alternative form for

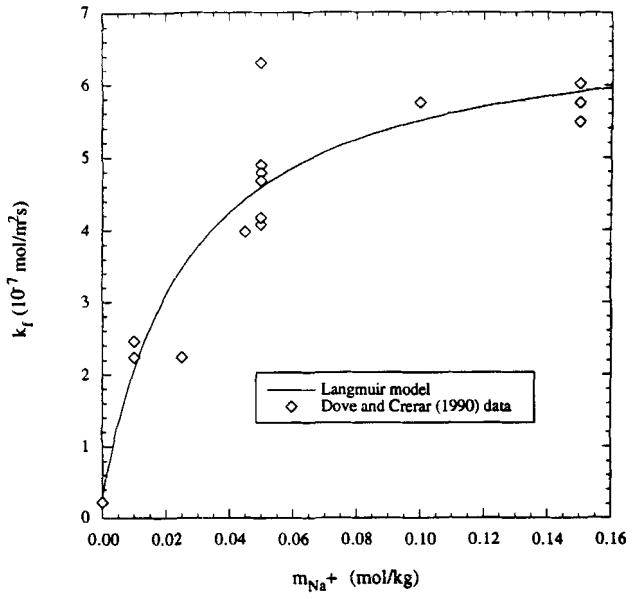


**Figure 14. Langmuir fit of the effect of $Na^+$ (NaCl added to deionized water) at 200°C on the quartz dissolution rate of quartz (Dove and Crerar, 1990).**

the absorption isotherm was proposed by Freundlich

$$\theta_A = g m_A^{1/n_f} \tag{11}$$

where $n_f$ and $g$ are empirical parameters that usually decrease with increasing temperature. Although the Freundlich isotherm was originally empirical, it can be derived both thermodynamically and statistically. The thermodynamic derivation treats $n_f$ as a constant correcting for the mutual interaction of the absorbed molecules. Experimental values of $n_f$ are usually greater than unity, implying that the forces between the adsorbed molecules are repulsive. The statistical derivation applies the Langmuir adsorption isotherm to a distribution of energies among sites such that the heat of adsorption decreases logarithmically with coverage. The form of the Freundlich isotherm (Eq. 11), suggests that $\theta_A$ increases indefinitely as $m_A$ increases; however, the statistical derivation implies a maximum value of $\theta_A$ which is related to the heat of adsorption.

Applying Eq. 11 to the first-order form ($n = 1$) of Eq. 8, yields the following rate equation

$$k_f = k_{\theta_A} g m_A^{1/n_f} \tag{12}$$

which is exactly analogous with the empirical rate laws presented earlier when either $m_{Na^+}$ or $m_{OH^-}$ are held constant, with $1/n_f$ corresponding to $b$ and $c$ for $m_A = m_{OH^-}$ and $m_{Na^+}$, respectively. Equation 12 does not lead to any further analysis, except for the qualitative trend seen in $1/n_f$. Typically, $n_f$ decreases with increasing temperature (Satterfield, 1980), which would imply that $b$ and $c$ will increase with increasing temperature. However, based on our data and available literature data, statistically significant trends in the $b$ and $c$ parameters are not justified.

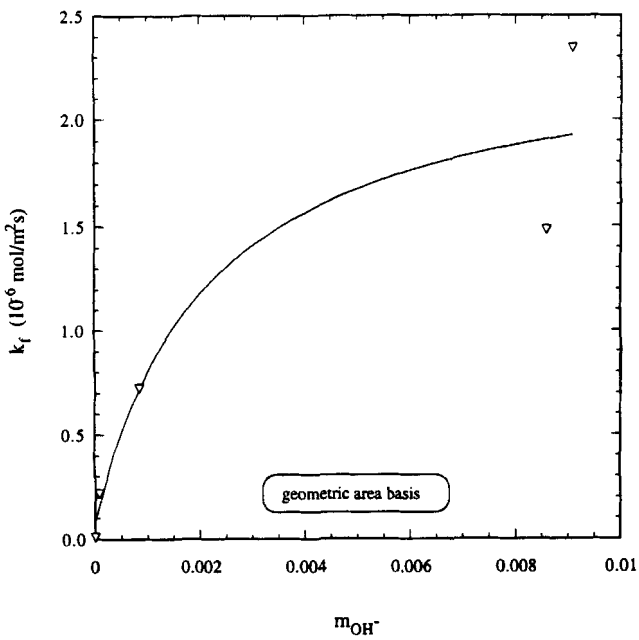


**Figure 15. Langmuir fit of the effect of $OH^-$ on 150°C quartz dissolution rates at constant $Na^+$ (this study).**

## Discussion

A general empirical correlation can be developed combining concepts developed in this study with those presented earlier in Tester et al. (1994), however, extrapolating trends seen at one set of experimental conditions to others is dangerous. A central objective of this study was not only to perform measurements under well-controlled conditions, but also to validate our data by comparing it with work performed by others.

### *pH effects*

A more comprehensive dissolution rate model (Eq. 5) was proposed which accounts for the effects of $OH^-$ and $Na^+$ (or ionic strength in deionized water) concentration

$$k_f = k_{OH,I} m_{OH^-}^b I^c \tag{13}$$

Although this model was able to correlate our rate data well from 100 to 200°C and from deionized water to solutions with NaOH (0.01 molal) and NaCl (0.1 molal) added, the resulting fractional order kinetics arise due to the empirical nature of the model. A more robust model would be based on surface species as opposed to solution species; unfortunately, little is known about the surface concentrations on quartz at high temperatures. However, if our goal was solely to develop an empirical correlation to predict quartz dissolution rates over a range of temperature and solution concentration, then we only need to determine the Arrhenius parameters (activation energy and pre-exponential constant) and the apparent reaction orders (and possibly their temperature dependence) with respect to variations in solution composition.

### *Mechanistic implications for quartz dissolution*

While the global regressions and rate laws developed from these data correlate quartz dissolution rates, they only provide limited mechanistic information at a molecular level. Clearly, there is more fundamental information that can be extracted from the experimental data.

The similarities between the surface charge behavior of quartz and the dissolution rate of quartz at 25°C might suggest that surface charge plays a dominant role in the dissolution rate process. However, the results of Tester et al. (1994) indicate that accurate dissolution measurements at 25°C are difficult to carry out. Considering the scatter in the dissolution rate data and the surface charge data, one cannot conclusively say that the quartz dissolution is directly proportional to surface charge.

The activation energy for quartz dissolution ($72 \pm 6$ kJ/mol) is much lower than the Si-O bond energy of 228 kJ/mol (Robie et al., 1979). Therefore, some solution species or reaction intermediate must destabilize the quartz structure causing the activation energy to be much less than the Si-O bond energy. The hydroxide ion was shown to catalyze quartz dissolution since it increased the dissolution rate without being consumed in the reaction. This scenario is different than a heterogeneous catalysis effect where the solid substrate is the catalyst and the fluid phase contains the reactants. If the dissolution rate is found to be directly proportional to surface charge, we still cannot present a conclusive mechanism for quartz dissolution. The surface charge may be just a good indicator of an unknown reaction intermediate. The quartz surface charge at intermediate and high pH consists of terminal $Si\text{-}O^-$ bond as proposed by a number of investigators (Charles, 1958; Le Roux, 1965; Atkinson, 1979; Iler, 1987; White et al., 1987; Grigsby, 1989).

As direct experimental measurements of reaction intermediates in solid-liquid systems do not exist today, mechanisms of quartz dissolution are most likely to be limited to enlightened empiricism mixed with partially validated theoretical approximations. *Ab initio* quantum mechanical methods provide some molecular level insight into the mechanisms of quartz dissolution, however, there are many limitations and approximations employed in these approaches as well. Perhaps with more advanced computers and more realistic representations of intermolecular forces on quartz surfaces, we can gather better mechanistic information from these calculations.

## Conclusions

Quartz dissolution rates were measured from 100 to 200°C over a wide range of pH and ionic strength. The dissolution rates in acidic $HNO_3$ solutions were slower than deionized water rates at the same temperature. At 175°C, the decline in dissolution rate levels off at approximately pH 3 and begins to increase again at pH 1 to 1.5. Addition of NaOH significantly enhanced the rate of quartz dissolution. The rate depended on the sodium ion concentration to the 0.26 power, while the hydroxide ion concentration dependence varied from 0.52 at 100°C to 0.62 at 200°C. This temperature variation was not statistically significant, especially when previous investigations were evaluated. If variations with temperature do exist, more accurate data needs to be obtained.

In the past, the activation energy of quartz dissolution was stated as being pH dependent (Brady and Walther, 1990). However, this occurs because a global model of quartz dissolution was used. In this study, the concentration dependence on the rate of dissolution was separated from the temperature dependence using a fractional order empirical rate law. The apparent activation energy in the empirical rate constant ($k_{OH,I}$ in Eq. 5) was found to be $72 (\pm 6)$ kJ/mol over a range of solution compositions from deionized water to an aqueous mixture of NaOH and NaCl at 0.01 molal $OH^-$ and 0.1 molal $Na^+$.

## Acknowledgment

We gratefully acknowledge the Hot Dry Rock geothermal energy program at Los Alamos National Laboratory and the Leopold Schepp Foundation for partial support of this project. Interactions with Bruce Robinson, Jeffrey Feerer, Robert Charles, Dale Counce, Theresa Bowers, David Duchane, James Albright, and Robert Potter were especially helpful. We are especially grateful to Professor Patricia Dove for her willingness to provide preprints of her work and for her critical analysis of our research results and its implications.

## Literature Cited

Armstead, H. C., and J. W. Tester, *Heat Mining*, E. and F. Spon, Section 10.4, London (1987).

Atkinson, B. K., "A Fracture Mechanics Study of Subcritical Tensile Cracking of Quartz in Wet Envirnoments," *Pageoph*, **117**, 1011 (1979).

Bennett, P. C., "Quartz Dissolution in Organic-Rich Aqueous Systems," *Geochim. Cosmochim. Acta*, **55**, 1781 (1991).

Berger, C., E. Cadere, J. Shott, and P. M. Dove, "Dissolution Rate of Quartz in Lead and Sodium Electrolyte Solutions between 25 and 300°C: Effect of the Nature of Surface Complexes and Reaction Affinity," *Geochim. Cosmochim. Acta*, **58**, 541 (1994).

Blum, A. E., and A. C. Lasaga, "Role of Surface Speciation in the Low-Temperature Dissolution of Minerals," *Nature*, **331**, 431 (1988).

Bolt, G. H., "Determination of the Charge Density of Silica Sols," *J. Phys. Chem.*, **61**, 1166 (1957).

Brady, P. V., "Silica Surface Chemistry at Elevated Temperatures," *Geochim. Cosmochim. Acta*, **56**, 2941 (1992).

Brady, P. V., and J. V. Walther, "Controls on Silicate Dissolution Rates in Neutral and Basic pH Solutions at 25°C," *Geochim. Cosmochim. Acta*, **53**, 2823 (1989).

Brady, P. V., and J. V. Walther, "Kinetics of Quartz Dissolution at Low Temperatures," *Chem. Geol.*, **82**, 253 (1990).

Charles, R. J., "Static Fatigue of Glass," *J. Applied Physics*, **29**, 1549 (1958).

Charles, R. W., "Experimental Geothermal Loop: II. 200°C Study," *Los Alamos Scientific Laboratory Report LA-7735-MS*, Los Alamos, NM (1979).

Charles, R. W., C. E. Holley, J. W. Tester, C. O. Grigsby, and L. A. Blatz, "Experimentally Determined Rock-Fluid Interactions Applicable to a Natural Hot Dry Rock Geothermal System," TMS Paper Selection Report A80-8, Metallurgical Soc. of AIME (1979).

Dove, P. M., "The Dissolution Kinetics of Quartz in Sodium Chloride Solutions at 25°C to 300°C," *Amer. J. Sci.*, **294**, 665 (1994).

Dove, P. M., and D. A. Crerar, "Kinetics of Quartz Dissolution in Electrolyte Solutions using a Hydrothermal Mixed Flow Reactor," *Geochim. Cosmochim. Acta*, **54**, 955 (1990).

Dove, P. M., and S. F. Elson, "The Low-Temperature Dissolution Kinetics of Quartz in Sodium Chloride Solutions: Analysis of Existing Data and a Rate Model for 25°C, pH 2-13," *Geochim. Cosmochim. Acta*, **56**, 4147 (1992).

Dove, P. M., and J. D. Rimstidt, "Silica-Water Interactions," *Rev. in Mineralogy Ser.: Silica Physical Behavior, Geochemistry, and Mat. Interactions*, **30**, 260 (1994).

Fleming, B. A., "Kinetics of Reaction between Silicic Acid and Amorphous Silica Surfaces in NaCl Solutions," *J. Colloid Interf. Sci.*, **110**(1), 40 (1986).

Fleming, B. A., and D. A. Crerar, "Silicic Acid Ionization and Calculation of Silica Solubility at Elevated Temperature and pH: Application to Geothermal Fluid Processing and Reinjection," *Geothermics*, **11**(1), 15 (1982).
Gratz, A. J., and P. Bird, "Quartz Dissolution: Negative Crystal Experiments and a Rate Law," *Geochim. Cosmochim. Acta*, **57**, 965 (1993).
Gratz, A. J., P. Bird and G. B. Quiro, "Dissolution of Quartz in Aqueous Basic Solution, 106–236°C: Surface Kinetics of 'Perfect' Crystallographic Faces," *Geochim. Cosmochim. Acta*, **54**, 2911 (1990).
Grigsby, C. O., "Kinetics of Rock-Water Reactions," PhD Thesis, Dept. of Chemical Engineering, Mass. Inst. of Technol., Cambridge (1989).
Grigsby, C. O., J. W. Tester, P. E. Trujillo, and D. A. Counce, "Rock-Water Interactions in the Fenton Hill, New Mexico, Hot Dry Rock Geothermal Systems: I. Fluid Mixing and Chemical Geothermometry," *Geothermics*, **18**(5/6), 629 (1989).
Hayes, K. F., and J. O. Leckie, "Modeling Ionic Strength Effects on Cation Adsorption at Hydrous Oxide/Solution Interfaces," *J. Colloid Interf. Sci.*, **115**, 564 (1987).
Helgeson, H. C., "Thermodynamics of Complex Dissociation in Aqueous Solution at Elevated Temperatures," *J. Phys. Chem.*, **71**(10), 3121 (1967).
Helgeson, H. C., "Thermodynamics of Hydrothermal Systems at Elevated Temperatures and Pressures," *Amer. J. Sci.*, **267**, 729 (1969).
Helgeson, H. C., D. H. Kirkham, and G. C. Flowers, "Theoretical Prediction of the Behavior of Aqueous Electrolytes at High Pressures and Temperatures: Calculation of Activity Coefficients, Osmotic Coefficients, and Apparent Molal and Standard and Relative Partial Molar Properties to 600°C and 5 kb," *Amer. J. Sci.*, **281**, 1249 (1981).
Helgeson, H. C., W. M. Murphy, and P. Aagaard, "Thermodynamic and Kinetic Constraints on Reaction Rates among Minerals and Aqueous Solutions: II. Rate Constants, Effective Surface Area, and the Hydrolysis of Feldspar," *Geochim. Cosmochim. Acta*, **48**, 2405 (1984).
House, W. A., and D. R. Orr, "Investigation of the pH Dependence of the Kinetics of Quartz Dissolution at 25°C," *J. Chem. Soc. Faraday Trans.*, **88**(2), 233 (1992).
Iler, R., *The Chemistry of Silica*, Wiley, New York (1987).
Kamiya, H., A. Ozaki, and M. Imahashi, "Dissolution Rate of Powered Quartz in Acid Solution," *Geochem. J. (Japan)*, **8**, 21 (1974).
Kita, H., N. Henmi, K. Shimazu, H. Hattori, and K. Tanabe, "Measurement of Acid-Base Properties on Metal Oxide Surfaces in Aqueous Solution," *J. Chem. Soc. Farad. Trans. I*, **77**, 2451 (1981).
Kline, W. E., and H. S. Fogler, "Dissolution Kinetics: Catalysis by Salts," *J. Colloid Interf. Sci.*, **82**, 103 (1981a).
Kline, W. E., and H. S. Fogler, "Dissolution Kinetics: Catalysis by Strong Acids," *J. Colloid Interf. Sci.*, **82**, 93 (1981b).
Knauss, K. G., and T. J. Wolery, "The Dissolution Kinetics of Quartz as a Function of pH and Time at 70°C," *Geochim. Cosmochim. Acta*, **52**, 43 (1988).
Kuester, J. L., and J. H. Mize, *Optimization Techniques with FORTRAN*, McGraw-Hill, New York (1973).
Lasaga, A. C., "Transition State Theory," *Kinetics of Geochemical Processes*, Chap. 4, *Rev. Mineralogy*, **8**, 135 (1981).
Le Roux, H., "The Strength of Fused Quartz in Water Vapor," *Proc. Roy. Soc. of London, Ser. A*, **286**, 390 (1965).
Marshall, W. L., and R. Slusher, "The Ionization Constant of Nitric Acid at High Temperatures from Solubilities of Calcium Sulfate in $HNO_3$-$H_2O$, 100–350°C; Activity Coefficients and Thermodynamic Function," *I. Inorg. Nucl. Chem..*, **37**, 1191 (1975).
Maurer, G., "On the Solubility of Volatile Weak Electrolytes in Aqueous Solutions," *Thermodynamics of Aqueous Systems with Industrial Applications*, Washington, DC (1980).
O'Connor, T. L., and S. A. Greenberg, "The Kinetics for the Solutions of Silica in Aqueous Solutions," *J. Phys. Chem.*, **62**, 1195 (1958).
Rimstidt, J. D., and H. L. Barnes, "The Kinetics of Silica-Water Reactions," *Geochim. Cosmochim. Acta*, **44**, 1683 (1980).
Robie, R. A., B. S. Hemingway, and J. R. Fisher, "Thermodynamic Properties of Minerals and Related Substances at 298.15 K and 1 bar ($10^5$ Pascals) and at Higher Temperatures," U.S. Geological Survey Bulletin 1452 (1979).
Robinson, B. A., "Quartz Dissolution and Silica Deposition in Hot Dry Rock Geothermal Systems," MS Thesis, Dept. of Chemical Engineering, Mass. Inst. of Technol., Cambridge (1982).
Satterfield, C. N., *Heterogeneous Catalysis in Practice*, McGraw Hill, New York (1980).
Siebert, H., W. V. Youdelis, J. Leja, and E. O. Lilge, "The Kinetics of the Dissolution of Crystalline Quartz in Water at High Temperatures and Pressures," *Unit Processes in Hydrometall.*, **24**, 284 (1963).
Sposito, G., "On the Surface Complexation Model of the Oxide Aqueous Solution Interface," *J. Colloid Interf. Sci.*, **91**(2), 329 (1983).
Stumm, W., G. Furrer, E. Wieland, and B. Zinder, "The Effects of Complex-Forming Ligands on the Dissolution of Oxides and Aluminosilicates," *The Chemistry of Weathering*, D. Reidel Publishing Co., Rodez, France (1985).
Tester, J. W., C. E. Holley, and L. A. Blatz, "Solution Chemistry and Scaling in Hot Dry Rock Geothermal Systems," AIChE meeting (1977).
Tester, J. W., W. C. Worley, B. A. Robinson, C. O. Grigsby, and J. L. Feerer, "Correlating Quartz Dissolution Kinetics in Pure Water from 25 to 625°C," *Geochim. Cosmochim. Acta*, **58**, 2407 (1994).
Truesdell, A. H., "Introduction to Chemical Calculations," *Fluid-Mineral Equilibria in Hydrothermal Systems*, Soc. of Economic Geologists, El Paso, TX (1984).
Truesdell, A. H., and B. F. Jones, "WATEQ, a Computer Program for Calculating Chemical Equilibria of Natural Waters," *J. Res., U.S. Geological Survey*, **2**, 233 (1974).
van Lier, J. A., P. L. de Bruyn, and J. Th. Q. Overbeck, "The Solubility Quartz," *J. Phys. Chem.*, **64**, 1675 (1960).
Westall, J., and H. Hohl, "A Comparison of Electrostatic Models for the Oxide/Solution Interface," *Adv. Colloid Interf. Sci.*, **12**, 265 (1980).
White, G. S., S. W. Freiman, S. M. Widerhorm, and T. D. Coyle, "Effects of Counterions on Crack Growth in Vitreous Silica," *J. Amer. Ceram. Soc.*, **70**, 891 (1987).
Wirth, G. S., and J. M. Gieskes, "The Initial Kinetics of the Dissolution of Vitreous Silica in Aqueous Media," *J. Colloid Interf. Sci.*, **68**(3), 492 (1979).
Wollast, R., and L. Chou, "Processes, Rate, and Proton Consumption by Silicate Weathering," *Trans. Cong. Int. Soc. Soil Sci.*, 127 (1986).
Zemaitis, J. F., Jr., D. M. Clark, M. Rafal, and N. C. Scrivner, *Handbook of Aqueous Electrolyte Thermodynamics*, AIChE, New York (1986).

## Appendix

### *Thermodynamic speciation model*

The analysis of rate data requires the calculation of species concentrations at the reaction temperature. For example, if a given amount of NaOH is added to the feed tank, we would like to know the concentration of solution species inside the reactor. A spreadsheet model was developed to solve for the species distribution given dissociation relations and the extended Debye-Hückel equation (Zemaitis et al., 1986). In this section, we will state the assumptions in the model, set up the equations, and describe the iteration methodology.

The first item needed in this model is the equilibrium constants for all dissociation reactions. The equilibrium constants for $H_2O$, $H_2CO_3$, and $HCO_3^-$ and the Henry's Law constant for $CO_2$ were obtained using a four-parameter, extended van't Hoff empirical expression by Maurer (1980) of the following form

$$\ln K = p/T + q \ln T + rT + s \qquad \text{(A1)}$$

where $K$ is an equilibrium constant, $T$ is the temperature in Kelvins, and $p$, $q$, $r$, and $s$ are empirical fitting parameters. The values for $p$, $q$, $r$, and $s$ are listed in Table 6 for each species. The dissociation constant for $H_4SiO_4$, $K_{H_4SiO_4}$, was

**Table 6. Empirical Constants Used to Calculate Henry's Law and Dissociation Constants (from Maurer, 1980)**

| $\ln K = p/T + q \ln T + rT + s$ ($T$ in K) | | | | | |
|---|---|---|---|---|---|
| | $p$ | $q$ | $r$ | $s$ | Temp. (K) |
| $H_{CO_2}$ | −6,789.04 | −11.4519 | −0.010454 | 94.4914 | 273–523 |
| $K_{H_2O}$ | −13,445.9 | −22.4773 | 0 | 140.932 | 273–498 |
| $K_{H_2CO_3}$ | −12,092.1 | −36.7816 | 0 | 235.482 | 273–498 |
| $K_{HCO_3^-}$ | −12,431.7 | −35.4819 | 0 | 220.067 | 273–498 |

determined using the following relation developed by Fleming and Crerar (1982)

$$\log K_{H_4SiO_4} = (1{,}479/T - 0.6496) + \log K_{H_2O} \qquad \text{(A2)}$$

where $T$ is in Kelvins. Finally, the dissociation constant for NaOH, $K_{NaOH}$, was taken from Helgeson (1967), however, under the conditions encountered in this study, NaOH is essentially 100% dissociated. NaCl and $Na_2SO_4$ were assumed to be completely dissociated, which should be a good assumption for the conditions in this study.

The following equations come directly from the assumption of equilibrium between the ionic species and their undissociated counterparts

$$K_{H_2O} = \frac{a_{H^+} a_{OH^-}}{a_w} \qquad \text{(A3)}$$

where $a_w$ = water activity $\cong 1.0$ and

$$K_{H_2CO_3} = \frac{a_{H^+} a_{HCO_3^-}}{a_{H_2CO_3}} \qquad \text{(A4)}$$

$$K_{HCO_3^-} = \frac{a_{H^+} a_{CO_3^=}}{a_{HCO_3^-}} \qquad \text{(A5)}$$

$$K_{NaOH} = \frac{a_{Na^+} a_{HO^-}}{a_{NaOH}} \qquad \text{(A6)}$$

$$K_{H_4SiO_4} = \frac{a_{H^+} a_{H_3SiO_4^-}}{a_{H_4SiO_4}} \qquad \text{(A7)}$$

where the activity of species $i$, $a_i$, can be written as the product of the concentration of species $i$, (mol $i$/kg $H_2O$) $m_i$, and the activity coefficient of species $i$, $\gamma_i$

$$a_i = \gamma_i m_i \qquad \text{(A8)}$$

The standard states are defined as unit molality (mol/kg $H_2O$) at the system temperature. In this model we will assume that the activity coefficients for undissociated species are unity, and the extended Debye-Hückel equation (discussed later in this section) describes the activity coefficient of ionic species.

Now we can eliminate activities from Eqs. A3 to A7. For example, for NaOH

$$K_{NaOH} = \frac{a_{Na^+} a_{OH^-}}{a_{NaOH}} = \gamma_{Na^+}\gamma_{OH^-}\frac{m_{Na^+} m_{OH^-}}{m_{NaOH}} \qquad \text{(A9)}$$

The total amount of sodium in mol/kg $H_2O$, $\Sigma$Na, is known from the amount of NaOH added. However, we need to determine $m_{Na^+}$ and $m_{NaOH}$.

$$\Sigma\text{Na} = m_{NaOH} + m_{Na^+} \qquad \text{(A10)}$$

Solving Eq. A9 for $m_{NA^+}$, yields

$$m_{Na^+} = \frac{K_{NaOH} m_{NaOH}}{\gamma_{Na^+}\gamma_{OH^-} m_{OH^-}} \qquad \text{(A11)}$$

Substituting Eq. A10 for $m_{NaOH}$ into Eq. A11, gives

$$m_{Na^+} = \frac{K_{NaOH}(\Sigma\text{Na} - m_{Na^+})}{\gamma_{Na^+}\gamma_{OH^-} m_{OH^-}} \qquad \text{(A12)}$$

or by rearrangement

$$m_{Na^+} = \frac{K_{NaOH}\Sigma\text{Na}}{(\gamma_{Na^+}\gamma_{OH^-} m_{OH^-} + K_{NaOH})} \qquad \text{(A13)}$$

Now, once we know the activity coefficients and $m_{OH^-}$, we can calculate $m_{Na^+}$. A similar equation can be derived for $m_{H_2SiO_4^-}$ since the total amount of dissolved silica $\Sigma$Si is known from solution analysis

$$m_{H_3SiO_4^-} = \frac{K_{H_4SiO_4}\Sigma\text{Si}}{(\gamma_{H^+}\gamma_{H_3SiO_4^-} m_{H^+} + K_{H_4SiO_4})} \qquad \text{(A14)}$$

The same approach is taken for the carbon balance, although there are two main differences: First, there are three carbon species in solution such that

$$\Sigma C = m_{H_2CO_3} + m_{HCO_3^-} + m_{CO_3^=} \qquad \text{(A15)}$$

and second, the total $CO_2$ in solution is not simply added or measured. The carbonic acid concentration depends on the Henry's law constant for $CO_2$, $H_{CO_2}$ in the following manner

$$m_{H_2CO_3} = P_{CO_2}/H_{CO_2} \qquad \text{(A16)}$$

This equation only applies to equilibrium conditions. The solutions used in this study are not necessarily at equilibrium and $P_{CO_2}$ is not known since the feed tank is sparged with nitrogen. The normal starting procedure for a run consists of adding acid or base to feed tank water that is in equilibrium with atmospheric $CO_2$. At this pH, $CO_2$ is highly soluble so the feed tank is sparged to maintain the total $CO_2$ approximately equal to its starting value. To model this process, we assume that the total $CO_2$ in solution is equal to $m_{H_2CO_3}$ of the starting solution

$$\Sigma C = P_{CO_2}/H_{CO_2} \qquad \text{(A17)}$$

$P_{CO_2}$ is taken initially as 0.00035 atm (350 ppm $CO_2$). $P_{CO_2}$ (or $\Sigma C$) will be used as an adjustable parameter since the nitrogen sparging may increase or decrease the total $CO_2$

concentration from its initial value. Now that we have an estimate for the total $CO_2$ in solution, we can follow a similar approach used in the derivation of Eq. A13.

Using the equilibrium relations and substituting for $m_{H_2CO_3}$ and $m_{CO_3^=}$ in Eq. A15, we get, for the total carbon in solution

$$\Sigma C = \frac{\gamma_{H^+}\gamma_{HCO_3^-} m_{H^+} m_{HCO_3^-}}{K_{H_2CO_3}} + m_{HCO_3^-} + \frac{\gamma_{HCO_3} m_{HCO_3^-} K_{HCO_3^-}}{\gamma_{H^+}\gamma_{CO_3^=} m_{H^+}} \quad \text{(A18)}$$

Solving for $m_{HCO_3^-}$

$$m_{HCO_3^-} = \Sigma C \left\{ \frac{\gamma_{H^+}\gamma_{HCO_3^-} m_{H^+}}{K_{H_2CO_3}} + 1 + \frac{\gamma_{HCO_3} K_{HCO_3^-}}{\gamma_{H^+}\gamma_{CO_3^=} m_{H^+}} \right\}^{-1} \quad \text{(A19)}$$

We can find $m_{CO_3^=}$ by substituting this result into the following equation

$$m_{CO_3^=} = \frac{\gamma_{HCO_3} m_{HCO_3^-} K_{HCO_3^-}}{\gamma_{H^+}\gamma_{CO_3^=} m_{H^+}} \quad \text{(A20)}$$

and $m_{H_2CO_3}$ can be found from a carbon balance in Eq. A15

$$m_{H_2CO_3} = \Sigma C - m_{HCO_3^-} + m_{CO_3^=} \quad \text{(A21)}$$

$m_{H^+}$ can be determined from the dissociation of water

$$m_{H^+} = \frac{K_{H_2O}}{\gamma_{H^+}\gamma_{OH^-} m_{OH^-}} \quad \text{(A22)}$$

Now assuming that we can calculate the activity coefficients, the preceding equations specify all of the species concentrations except for $m_{OH^-}$. The final equation is the charge balance which can be used to calculate $m_{OH^-}$

$$m_{OH^-} = m_{H^+} + m_{Na^+} - m_{HCO_3^-} - 2m_{CO_3^=} - m_{H_3SiO_4^-} \quad \text{(A23)}$$

Equation A23 will change slightly if NaCl or $Na_2SO_4$ is added to the solution, however, since these salts are essentially 100% dissociated, no other adjustments to the model are needed.

The algorithm used to solve these equations is simple. First, a value of $m_{OH^-}$ and the total ionic strength are guessed. The ionic strength is used to calculate the activity coefficient of each species using the extended Debye-Hückel equation.

Equations A13, A14, A19, A20, and A22 are used to calculate $m_{Na^+}$, $m_{H_3SiO_4^-}$, $m_{HCO_3^-}$, $m_{CO_3^=}$, and $m_{H^+}$, respectively. Now we can iterate $m_{OH^-}$ until the charge balance (Eq. A23) is satisfied. At this point, the ionic strength is recalculated, the activity coefficients are determined from the extended Debye-Hückel equation, and we can iterate on $m_{OH^-}$ again until the charge balance (Eq. A23) is satisfied. The conversion of this method is very fast, requiring only two iterations on $m_{OH^-}$.

The exact same algorithm is used in the low pH model, except now $HNO_3$ is used to adjust pH as opposed to NaOH. For this model, $m_{H^+}$ is used as the iteration variable instead of $m_{OH^-}$. A correlation for the dissociation constant of $HNO_3$ was taken from Marshall and Slusher (1975)

$$\log K_{HNO_3} = 74.925 - 6{,}204/T - 0.300649\,T + 5.15\times10^{-4}T^2 - 3.33\times10^{-7}T^3 \quad \text{(A24)}$$

where $T$ is in Kelvins. Although this correlation was based on data from 100 to 350°C, it agrees well with 25°C data.

## Extended Debye-Hückel Equation

An extended Debye-Hückel equation was used in our model due to its simplicity and ability to estimate activity coefficients reasonably accurately for the solutions used in this study over concentration ranges of interest. The form of the equation taken from Truesdell (1984) is as follows:

$$\log \gamma_i = \frac{Az_i^2\sqrt{I}}{1 + \alpha_i B\sqrt{I}} + \beta I \quad \text{(A25)}$$

where $z_i$ is the ionic charge of species $i$, $I$ is the ionic strength, and $A$, $B$, $\alpha_i$, $\beta$ are constants. $A$ and $B$ are related to the properties of the solvent and were taken from the values suggested by Helgeson et al. (1981). $\alpha_i$ represents the distance of closest approach between specified ions. Values of $\alpha_i$ used in our model are taken from Truesdell and Jones (1974), which are commonly used in geothermal fluid-mineral calculations. The $\beta I$ term was added by Hückel to account for the reduction of the dielectric constant by increased concentration (Zemaitis et al., 1986). Up to 250°C , $\beta$ has values in the range of 0.03 to 0.05 kg/mol when concentrations are as high as 3 molal (Helgeson, 1969). The value of $\beta$ used is assumed to be 0.04 kg/mol in our model. The value of the activity coefficient is very insensitive to the choices of $\alpha_i$ and $\beta$ for the ionic strength ranges of this study.

*Manuscript received Mar. 13, 1995, and revision received June 5, 1996.*